

## Controlled Synthesis of Palladium Nanocubes as an Efficient Nanocatalyst for Suzuki-Miyaura Cross-Coupling and Reduction of p-Nitrophenol

Swarnalata Swain, Bhavya M B, Vishal Kandathil, Prangya Bhol, Akshaya K Samal, and Siddappa A Patil

*Langmuir*, Just Accepted Manuscript • DOI: 10.1021/acs.langmuir.0c00526 • Publication Date (Web): 22 Apr 2020

Downloaded from pubs.acs.org on April 23, 2020

### Just Accepted

“Just Accepted” manuscripts have been peer-reviewed and accepted for publication. They are posted online prior to technical editing, formatting for publication and author proofing. The American Chemical Society provides “Just Accepted” as a service to the research community to expedite the dissemination of scientific material as soon as possible after acceptance. “Just Accepted” manuscripts appear in full in PDF format accompanied by an HTML abstract. “Just Accepted” manuscripts have been fully peer reviewed, but should not be considered the official version of record. They are citable by the Digital Object Identifier (DOI®). “Just Accepted” is an optional service offered to authors. Therefore, the “Just Accepted” Web site may not include all articles that will be published in the journal. After a manuscript is technically edited and formatted, it will be removed from the “Just Accepted” Web site and published as an ASAP article. Note that technical editing may introduce minor changes to the manuscript text and/or graphics which could affect content, and all legal disclaimers and ethical guidelines that apply to the journal pertain. ACS cannot be held responsible for errors or consequences arising from the use of information contained in these “Just Accepted” manuscripts.

# Controlled Synthesis of Palladium Nanocubes as an Efficient Nanocatalyst for Suzuki-Miyaura Cross-Coupling and Reduction of *p*-Nitrophenol

Swarnalata Swain,<sup>†</sup> Bhavya M. B.,<sup>†</sup> Vishal Kandathil, Prangya Bhol, Akshaya K. Samal,\*

Siddappa A. Patil\*

Centre for Nano and Material Sciences, Jain University, Jain Global Campus, Kanakapura,

Ramanagaram, Bangalore 562112, India

Email: s.akshaya@jainuniversity.ac.in, p.siddappa@jainuniversity.ac.in

## Abstract

Anisotropic nanocatalysts have attracted a considerable attention in comparison to bulk/nano catalysts for their enhanced activity and reactivity. The demand towards anisotropic palladium (Pd) nanostructures have been increased rapidly in the area of catalysis. Pd is a well-known active catalyst for several carbon-carbon (C-C) cross-coupling reactions, among them Suzuki-Miyaura cross-coupling reaction is one of the most versatile and dominant method for constructing the extraordinarily useful unsymmetrical biaryls and also for hydrogenation of organic contaminant like *p*-nitrophenol (*p*-NP). This paper provides a brief explanation about the controlled synthesis, characterization and catalytic activity of well defined palladium nanocubes (Pd NCs) prepared by the seed mediated method. The synthesized monodispersed Pd NCs were characterized by spectroscopic and microscopic tools such as UV-Visible, XRD, FESEM, HRTEM and EDS analyses. Pd NCs proved as an efficient catalyst for Suzuki-Miyaura cross-coupling reactions and *p*-NP reduction. The catalyst shows enhanced activity, greater stability and higher selectivity with remarkable recyclability upto 92% for five consecutive cycles. The catalytic performance of the synthesized Pd NCs have also studied in the reduction of the organic contaminant *p*-NP which showed an excellent performance screening of 99 % conversion in 6 minutes.

**Keywords:** Pd Nanocubes; C-C coupling reaction; Suzuki-Miyaura cross-coupling; Anisotropic nanostructures; *p*-Nitrophenol reduction.

## Introduction

Anisotropic nanostructures have emerged as a significant research area due to the unusual, enriched and unique properties associated with it and attracts new fundamental applications in the field of health, energy, water and environmental research. The structural features of anisotropic nanostructures play an important role, due to the shape, size and the enhanced selectivity and activity based on morphology. Isotropic nanoparticles have only one uniform surface to provide its activity but anisotropic nanostructures obtain asymmetric axes, and this transformation in symmetry is responsible for the enhanced properties of the synthesized nanocrystals.<sup>1,2</sup> Several approaches

1  
2  
3 have been employed for the synthesis of anisotropic nanostructures such as template assisted  
4 synthesis, electrochemical synthesis and photochemical synthesis etc. Synthesis of Pd tetrahedral  
5 and trigonal bipyramidal nanocrystals with concave surfaces using solvothermal process in the  
6 presence of formaldehyde has been performed.<sup>3-6</sup> Xia et al. successfully used polyol based synthesis  
7 in the presence of poly(vinyl pyrrolidone) (PVP) to form varieties of Pd nanostructures such as  
8 nanobars, short nanorods, nanocubes, octahedra, icosahedra, and nanoplates.<sup>7,8</sup> In spite of these  
9 reported procedures, it is simpler and easier to follow water-based seed mediated synthesis due to  
10 high yield and better control over the size and shape evolution of metal nanostructures.<sup>9,10</sup> In this  
11 paper, we report the synthesis of structurally well-defined monodisperse Pd nanostructures using  
12 seed mediated wet chemical synthesis. Cetyltrimethylammonium bromide (CTAB) used as capping  
13 or stabilizing agent in order to prevent the agglomeration during the formation of Pd NCs. Pd is  
14 well known catalyst for catalysing many industrial applications from a long time. Literature shows  
15 60% of Pd used as catalyst instead of Pt noble metal catalyst to minimize the cost effect and serves  
16 as an efficient metal substitution instead of Pt for performing various applications.<sup>11-17</sup> Some of the  
17 notable applications of Pd materials include sensing through surface enhanced Raman Scattering  
18 (SERS),<sup>18-21</sup> hydrogenation/dehydrogenation reactions, low-temperature reduction of automobile  
19 pollutants, and petroleum cracking.<sup>22-24</sup> Among all applications performed using Pd as a catalyst,  
20 C-C bond formation reactions has been attracted worldwide attention. Some of the examples of C-  
21 C bond forming reactions are Suzuki-Miyaura, Mizoroki-Heck, and Stille, Hiyama and Negishi  
22 cross-coupling reactions.<sup>25-28</sup> The biaryl products obtained plays characteristics role for the  
23 production of polymers, agrochemicals, pharmaceutical intermediates and high-tech materials.  
24 Suzuki-Miyaura cross-coupling reactions of aryl boronic acids with aryl halides recommend a  
25 valuable procedure to get biaryl compounds. This well-known reaction is mainly associated because  
26 of the utilization of mild reaction conditions and their tolerance towards wide variety of functional  
27 groups.<sup>29-33</sup> Balanta et al. elucidated a broad explanation towards Pd nanoparticles catalyzed C-C  
28 bond-forming processes, taking into account the recent work progress in this area and looking into  
29 stabilizing agent's performance, catalytic upshot and recycling prospective.<sup>34</sup> A wide summary of  
30 nanocatalysts for Suzuki-Miyaura cross-coupling reactions, emphasizing their performance,  
31 stability and recyclability has reported.<sup>35-38</sup> In this article, controlled growth of monodisperse Pd  
32 NCs along (100) plane attributed excellent catalytic behaviour for Suzuki-Miyaura cross-coupling  
33 reaction and 99% conversion for *p*-NP reduction. Being heterogeneous in nature, Pd NCs catalyst  
34 can be recovered easily from the reaction mixture and recycled for further rounds of analogous  
35 organic transformations. It has been observed that Pd NCs shows high product yields even for five  
36  
37  
38  
39  
40  
41  
42  
43  
44  
45  
46  
47  
48  
49  
50  
51  
52  
53  
54  
55  
56  
57  
58  
59  
60

consecutive cycle of reaction, suggesting that this can serve as an excellent recyclable catalyst. *p*-NP is one of the harmful contaminants among the organic pollutants. In living organisms, it is recognized for causing adverse health issues. The anthropogenic and toxic *p*-NP is used for manufacturing most of the pesticides, insecticides, fungicides and also used in case of hair dyes, pharmaceuticals purpose and to darken leather.<sup>39,40</sup> Human exposure to *p*-NP takes place by three pathways, namely inhalation, ingestion (eating, drinking) and dermal contact. Immediate exposure of *p*-NP by the pathways of inhalation or ingestion causes symptoms such as headaches, drowsiness, nausea, and cyanosis.<sup>41</sup> *p*-NP has the property of highly solubilized and more stable in water bodies which creates adverse effect for marine organisms. Hence, it is difficult to remove *p*-NP from contaminated waste water by traditional waste water treatment. Therefore, researchers have been used many techniques for the removal of *p*-NP. The techniques such as adsorption, microwave-assisted catalytic oxidation, microbial degradation, photo catalytic degradation, electro coagulation, and electrochemical treatment.<sup>42-45</sup> On the other hand, all these techniques have some drawbacks like energy-consuming and include the use of organic solvents. Therefore, in the present scenario, it is very important to develop and employ aqueous phase conversion of *p*-NP to *p*-AP under mild conditions by catalytic reduction method. The product (*p*-AP) obtained from the catalytic reduction of *p*-NP is effective in many useful applications such as analgesic and antipyretic drugs, photographic developer, corrosion inhibitor, anticorrosion lubricant etc..<sup>46</sup>

## Experimental

### Materials and methods

Palladium chloride, Cetyltrimethylammonium bromide, *p*-nitrophenol and NaBH<sub>4</sub> were purchased from SD Fine Chemical Limited, India and used without further purification. Ascorbic acid (L-AA) was purchased from Merck. All the glass wares were cleaned with aqua regia and finally rinsed with deionized water. UV-Visible analysis was carried out with the help of PerkinElmer Lambda 360 UV-Visible spectrophotometer. FESEM analysis was done with the instrument JEOL, Singapore. TEM and HRTEM measurements were carried out using Thermo Scientific TALOS F200S G2 (200 KV), FEG, CMOS Camera 4K x 4K. Samples for HRTEM were prepared by drop casting on 300 mesh carbon coated copper grid. XRD analysis was performed using the instrument Rigaku Ultima-IV from Japan. The unit cell parameters can be calculated from the formula  $a_0 = 2d_{10}/\sqrt{3}$ . The metallic Pd sizes can be estimated using Scherrer formula:  $\text{size} = 0.89\lambda/\beta \cos \theta$ .<sup>47</sup> Zeta potential and DLS (Dynamic Light Scattering) measurement were performed using Anton Paar Lite sizer 500 particle size analyser. <sup>1</sup>H NMR spectra were recorded at 400 MHz in deuterated

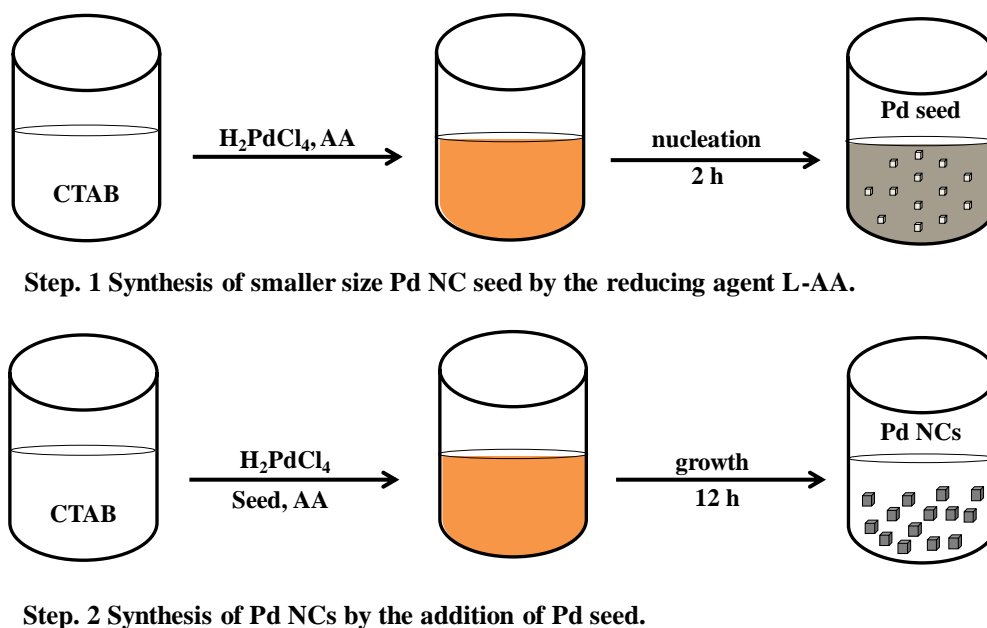
1  
2  
3 chloroform ( $\text{CDCl}_3$ ,  $\delta = 7.27$  ppm).  $^1\text{H}$  NMR coupling constants ( $J$ ) are reported in Hertz (Hz) and  
4 multiplicities are given as follows: s (singlet), d (doublet), t (triplet), m (multiplet).  
5  
6  
7

### 8 **Preparation of Pd seed**

9 Pd NCs are synthesized using seed mediated protocol with slight modification in the temperature  
10 reported by Anna Klinkova's group.<sup>48</sup> Initially,  $\text{H}_2\text{PdCl}_4$  (20 mM) was prepared by taking 0.115 g  
11 of  $\text{PdCl}_2$  with 6.5 mL 0.2 M conc. HCl and stirred for 3 h to obtain a clear orange solution of  
12  $\text{H}_2\text{PdCl}_4$ , followed by dilution with distilled water to make 20 mM  $\text{H}_2\text{PdCl}_4$  solution. For the  
13 synthesis of seed solution; 0.045 g CTAB was dissolved in 10 mL of distilled water in a 25 mL  
14 round bottom flask equipped with a stirring bar and heated to 95 °C under stirring for 5-10 min.  
15 After that, 0.25 mL of  $\text{H}_2\text{PdCl}_4$  was added followed by the addition of 0.02 mL of ascorbic acid (0.4  
16 M) solution at a stretch. The reaction mixture was stirred for 10 minutes and then cooled to 30 °C.  
17 The solution kept undisturbed 2 h for the complete growth of seed particles (Figure 1, step 1). The  
18 solution turns blackish brown from light orange.  
19  
20  
21  
22  
23  
24  
25  
26  
27

### 28 **Preparation of growth solution**

29 9.0 g of CTAB taken in a round bottom flask containing 90 mL of distilled water and stirred for 10-  
30 15 min at 70 °C. 3.2 mL of 20 mM  $\text{H}_2\text{PdCl}_4$  was added to it. Then, 2 mL of aged Pd seeds were  
31 added for the growth solution under vigorous stirring, followed by the addition of 2.5 mL of 0.4 M  
32 ascorbic acid. The resulting reaction mixture was kept undisturbed 12 h at 70 °C for the growth of  
33 Pd NCs. The resulting Pd NCs were settled at the bottom of the flask and the solution was sonicated  
34 for a minute to remove the settled particles from the flask (Figure 1, step 2). Then it was centrifuged  
35 twice at 6500 rpm for 15 minutes to remove the unreacted ions and excess surfactant. The residue  
36 was redispersed in deionised water and dried at 70 °C over night for further characterization.  
37  
38  
39  
40  
41  
42  
43  
44  
45  
46  
47  
48  
49  
50  
51  
52  
53  
54  
55  
56  
57  
58  
59  
60



23 **Figure 1.** Schematic representation of synthesis protocol of nucleation and growth of nuclei into  
24 desired Pd NCs.  
25

### 26 Procedure for Suzuki-Miyaura cross-coupling reaction

27  
28  
29  
30 To a mixture of aryl halide (1 equiv.), phenylboronic acid (1.1 equiv.), and potassium carbonate  
31 (2.2 equiv.) in ethanol:water (EtOH:H<sub>2</sub>O) (1:1) solvent system, Pd NCs (4 wt%) were added and  
32 stirred at room temperature for designated hours. TLC was employed to evaluate the progress of  
33 the reaction. After the reaction completion, Pd NCs were separated through centrifugation and the  
34 separated Pd NCs were washed with EtOH and water and then dried. To the filtrate,  
35 dichloromethane (DCM) and deionized water were added. DCM layer was separated from the water  
36 layer using a separating funnel and dried with sodium sulphate (Na<sub>2</sub>SO<sub>4</sub>). The separated DCM layer  
37 was concentrated in a rotary evaporator to obtain the crude product which was purified through  
38 column chromatography using hexane and ethyl acetate as eluting solvent to get the corresponding  
39 products in good to excellent yields. All the coupled products were reported molecules and were  
40 confirmed by comparing the <sup>1</sup>H NMR spectral data with those of the authentic samples.  
41  
42  
43  
44  
45  
46  
47  
48  
49

- 50  
51 1. *1,1'-Biphenyl* (Table 2, entries 1 & 11): Colourless crystals. <sup>1</sup>H NMR (400 MHz, CDCl<sub>3</sub>) δ 7.60  
52 (d, *J* = 7.4 Hz, 4H), 7.45 (t, *J* = 7.6 Hz, 4H), 7.35 (t, *J* = 7.3 Hz, 2H).  
53  
54 2. *[1,1'-Biphenyl]-4-ol* (Table 2, entries 2 and 12): Off-white solid. <sup>1</sup>H NMR (400 MHz, CDCl<sub>3</sub>) δ  
55 7.53 (d, *J* = 7.8 Hz, 2H), 7.47 (d, *J* = 8.6 Hz, 2H), 7.40 (t, *J* = 7.6 Hz, 2H), 7.29 (s, 1H), 6.90 (d, *J*  
56 = 8.6 Hz, 2H), 4.94 (s, 1H).  
57  
58  
59  
60

3. *[1,1'-Biphenyl]-2-carboxylic acid* (Table 2, entry 3): Off-white solid.  $^1\text{H}$  NMR (400 MHz,  $\text{CDCl}_3$ )  $\delta$  7.93 (d,  $J = 7.4$  Hz, 1H), 7.55 (d,  $J = 7.5$  Hz, 1H), 7.54 - 7.34 (m, 7H).
4. *4-Methyl-1,1'-biphenyl* (Table 2, entries 4 and 13): Colourless crystals.  $^1\text{H}$  NMR (400 MHz,  $\text{CDCl}_3$ )  $\delta$  7.57 (d,  $J = 7.5$  Hz, 2H), 7.48 (d,  $J = 8.1$  Hz, 2H), 7.41 (t,  $J = 7.6$  Hz, 2H), 7.32 (d,  $J = 7.3$  Hz, 1H), 7.23 (s, 2H), 2.39 (s, 3H).
5. *4-Methoxy-1,1'-biphenyl* (Table 2, entries 5 and 14): White solid.  $^1\text{H}$  NMR (400 MHz,  $\text{CDCl}_3$ )  $\delta$  7.47 (t,  $J = 9.3$  Hz, 4H), 7.34 (t,  $J = 7.3$  Hz, 2H), 7.23 (t,  $J = 7.2$  Hz, 1H), 6.90 (t,  $J = 9.6$  Hz, 2H), 3.78 (s, 3H).
6. *[1,1'-Biphenyl]-4-carbonitrile* (Table 2, entry 6): Pale yellow crystals.  $^1\text{H}$  NMR (400 MHz,  $\text{CDCl}_3$ )  $\delta$  7.72 (d,  $J = 8.4$  Hz, 2H), 7.67 (d,  $J = 8.4$  Hz, 2H), 7.60 – 7.56 (m, 2H), 7.48 (d,  $J = 10.0$  Hz, 2H), 7.42 (d,  $J = 8.4$  Hz, 1H).
7. *[1,1'-Biphenyl]-4-yl(phenyl)methanone* (Table 2, entry 7): Off-white solid.  $^1\text{H}$  NMR (400 MHz,  $\text{CDCl}_3$ )  $\delta$  7.89 (d,  $J = 8.3$  Hz, 2H), 7.86 – 7.81 (m, 2H), 7.70 (d,  $J = 8.3$  Hz, 2H), 7.65 (d,  $J = 7.3$  Hz, 2H), 7.60 (t,  $J = 7.4$  Hz, 1H), 7.49 (d,  $J = 7.8$  Hz, 4H), 7.40 (t,  $J = 7.3$  Hz, 1H).
8. *4-Nitro-1,1'-biphenyl* (Table 2, entry 8): Yellow crystals.  $^1\text{H}$  NMR (400 MHz,  $\text{CDCl}_3$ )  $\delta$  8.29 (d,  $J = 8.8$  Hz, 2H), 7.73 (d,  $J = 8.8$  Hz, 2H), 7.65 – 7.59 (m, 2H), 7.50 (d,  $J = 11.4$  Hz, 2H), 7.46 – 7.41 (m, 1H).
9. *1-([1,1'-Biphenyl]-4-yl)ethanone* (Table 2, entry 9): Off-white solid.  $^1\text{H}$  NMR (400 MHz,  $\text{CDCl}_3$ )  $\delta$  8.03 (d,  $J = 8.4$  Hz, 2H), 7.68 (d,  $J = 8.4$  Hz, 2H), 7.62 (d,  $J = 7.3$  Hz, 2H), 7.47 (t,  $J = 7.4$  Hz, 2H), 7.39 (t,  $J = 7.3$  Hz, 1H), 2.63 (s, 3H).
10. *[1,1'-Biphenyl]-2-carbaldehyde* (Table 2, entry 10): Pale yellow liquid.  $^1\text{H}$  NMR (400 MHz,  $\text{CDCl}_3$ )  $\delta$  9.98 (s, 1H), 8.02 (d,  $J = 7.8$  Hz, 1H), 7.64 (t,  $J = 7.5$  Hz, 1H), 7.52 – 7.41 (m, 5H), 7.38 (d,  $J = 7.5$  Hz, 2H).

### Procedure for *p*-NP to *p*-AP reduction

Further to investigate the catalytic activity of synthesized Pd NCs catalyst, a standard reduction test was carried out and the reaction progress was monitored through UV-Visible spectra. First, 0.01 M *p*-NP aqueous solution and 0.5 M  $\text{NaBH}_4$  solution were prepared and the reduction process was observed by the addition of synthesized Pd NCs. 20  $\mu\text{L}$  (0.01 M) *p*-NP was mixed with 3 mL of  $\text{H}_2\text{O}$  and then 10  $\mu\text{L}$  of ice-cold aqueous  $\text{NaBH}_4$  solution (0.5 M) was added which result in deep yellow colour solution. Then different amount of catalyst (mg/mL) was added to the reaction mixture and the progress of reaction was observed through UV-Visible analysis until the solution

1  
2  
3 became colourless. The maximum amount of reactant converted to product has been calculated by  
4 using the formula.<sup>49,50</sup>

$$\% \text{ reduction} = \frac{C_0 - C_t}{C_0} \times 100$$

8  
9 Where  $C_0$  is the initial concentration of phenolate ion and  $C_t$  is the concentration of phenolate ion  
10 at time  $t$ .

## 14 **Results and Discussion**

### 16 **Synthesis and characterization**

17  
18 Solution-phase synthesis of Pd NCs is typically conducted without using any inert environment. Pd  
19 precursor is reduced in the presence of stabilizer, CTAB. The overall synthesis protocol has been  
20 known as wet chemical seed mediated approach. Among all the synthetic methods, seed-mediated  
21 growth approach has been proven to be the finest method because it separates the nucleation and  
22 growth stages of nanoparticles, which provides better control over the size distribution, and shape  
23 evolution of nanoparticles. In this protocol, smaller size Pd NCs were formed as seed. These were  
24 synthesized through one-step reduction of  $\text{H}_2\text{PdCl}_4$  in aqueous solution with ascorbic acid in  
25 presence of CTAB at 95 °C. The colour of the solution turned to brownish black from light orange  
26 and it confirmed that the reduction process was rather fast at higher temperature (shown in Fig. 1).  
27 The reaction was kept undisturbed for 2 h to continue the aging process of the Pd seed. These seed  
28 particles were added to growth solution for the formation of Pd NCs with well distinct growth.  
29 FESEM images and corresponding histogram of the diagonal length of Pd NCs seed are given in  
30 Fig. 2(a) and 2(b), respectively. At ambient condition, a rapid reduction process was followed for  
31 the formation of smaller nuclei cubic Pd seeds. The seed nanocubes were produced in high yield  
32 and size of Pd NC seeds were  $22 \pm 5$  nm confirmed from the histogram shown in Fig. 2(b). Energy-  
33 dispersive X-ray spectroscopy (EDS) analysis used for the elemental analysis of desired samples in  
34 a selected surface area and provides information about the existence of each elements present in the  
35 sample. EDS has been performed for the seed nanocubes as shown in Fig. 2(c). The characteristic  
36 signals revealed the presence of Pd in the Pd NCs and inset shows the approximate wt. % and atomic  
37 % obtained from the corresponding FESEM image. The above characterized smaller size Pd seed  
38 particles were then injected into the reaction mixture during the preparation of growth solution for  
39 the formation of well grown Pd NCs in high yield by the help of stabilizing agent. Twinning of the  
40 nanostructures were completely avoided starting from nucleation stage to the growth process. The  
41 facets of Pd NCs proceeding at relatively lower temperatures has been reported previously.<sup>51</sup>

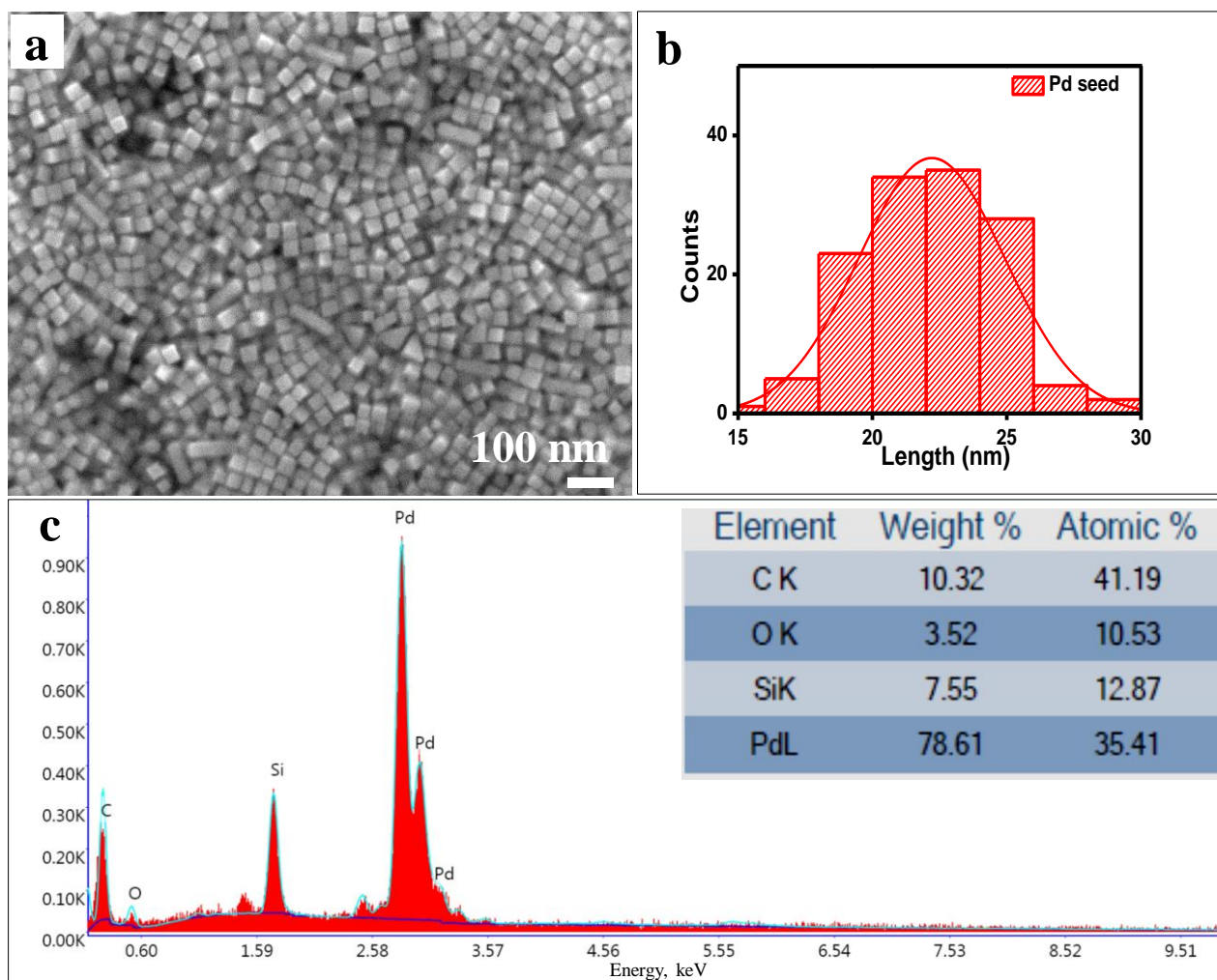


**Figure 2.** (a) FESEM image of cubic Pd seed particles, (b) corresponding histogram of seed particles shows the average size around  $22 \pm 5$  nm and (c) EDS analysis small cubic seed confirming the elements present in the selected area.

The growth Pd NCs were performed at  $70^\circ\text{C}$  using 20 mM  $\text{H}_2\text{PdCl}_4$  solution in presence of ascorbic acid as reductant. With slight modification in the temperature, multilayer and monodisperse formation of desired nanostructure was obtained in high yield compared to the previous report.<sup>48-51</sup> The obtained Pd NCs were purified using centrifugation after 12 h of cooling as discussed in the experimental section. Synthesized Pd NCs were preliminarily subjected to UV-Vis analysis. Fig. 3(a) represents the UV-Visible spectrum shows one broad peak of Pd NCs having  $\lambda_{\text{max}}$  at 416 nm. The peak position Pd NCs shift towards higher wavelength (bathochromic shift) or lower wavelength (hypsochromic shift) depending upon the size of the Pd NCs formed. Well defined, uniform size and shapes of Pd NCs are formed using smaller Pd seeds as mentioned wet chemical seed-mediated growth approach. FESEM analysis was carried out for Pd NCs on silicon wafer and

sonicated before the drop casting for better dispersity as shown in Fig. 3(b) and 3(c) which shows monodisperse morphology of Pd NCs. FESEM images show the multilayer formation and well dispersity of the sample. The diagonal length of the synthesized Pd NCs was  $60 \pm 5$  nm as shown in the histogram in Fig. 3(d). The characteristic signals observed for Pd NCs from EDS analysis represented in Fig. S1. The hydrodynamic diameter of the particles was found to be 126.25 nm from dynamic light scattering (DLS) measurement. To confirm the surface charge of Pd NCs, Zeta potential measurement was carried out. Zeta potential of Pd NCs was +41.4 mV due to the presence of cationic surfactant, CTAB. DLS and Zeta potential data were presented in the supporting information S2 and S3, respectively. The zeta potential of CTAB was found +44.4 mV and decreased in the case of Pd NCs.

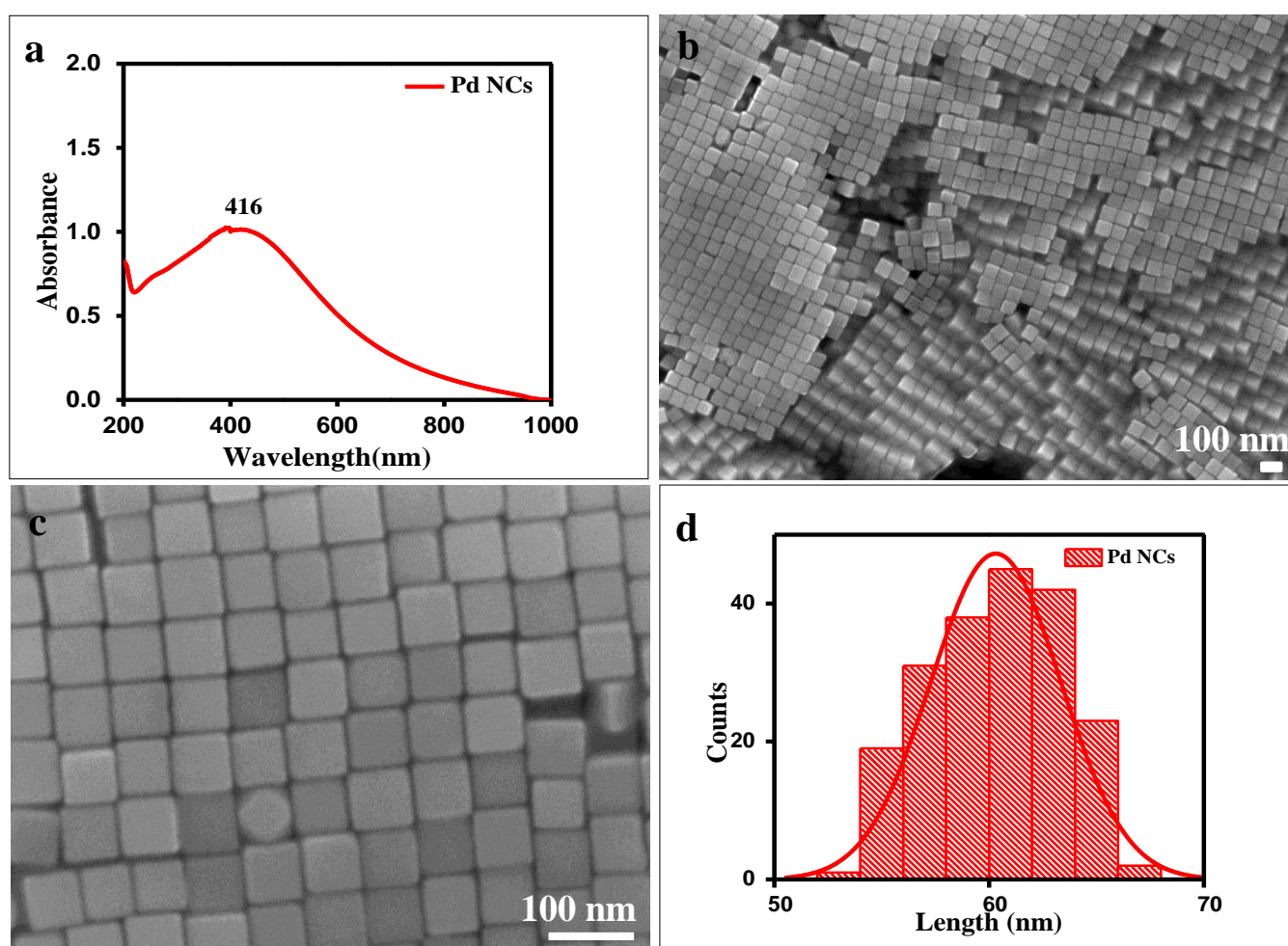


**Figure 3.** (a) UV-Visible spectrum of Pd NCs, (b) FESEM image Pd NCs showing multilayer growth, (c) high resolution FESEM image of monodispersed Pd NCs, (d) size distribution histogram of Pd NCs.

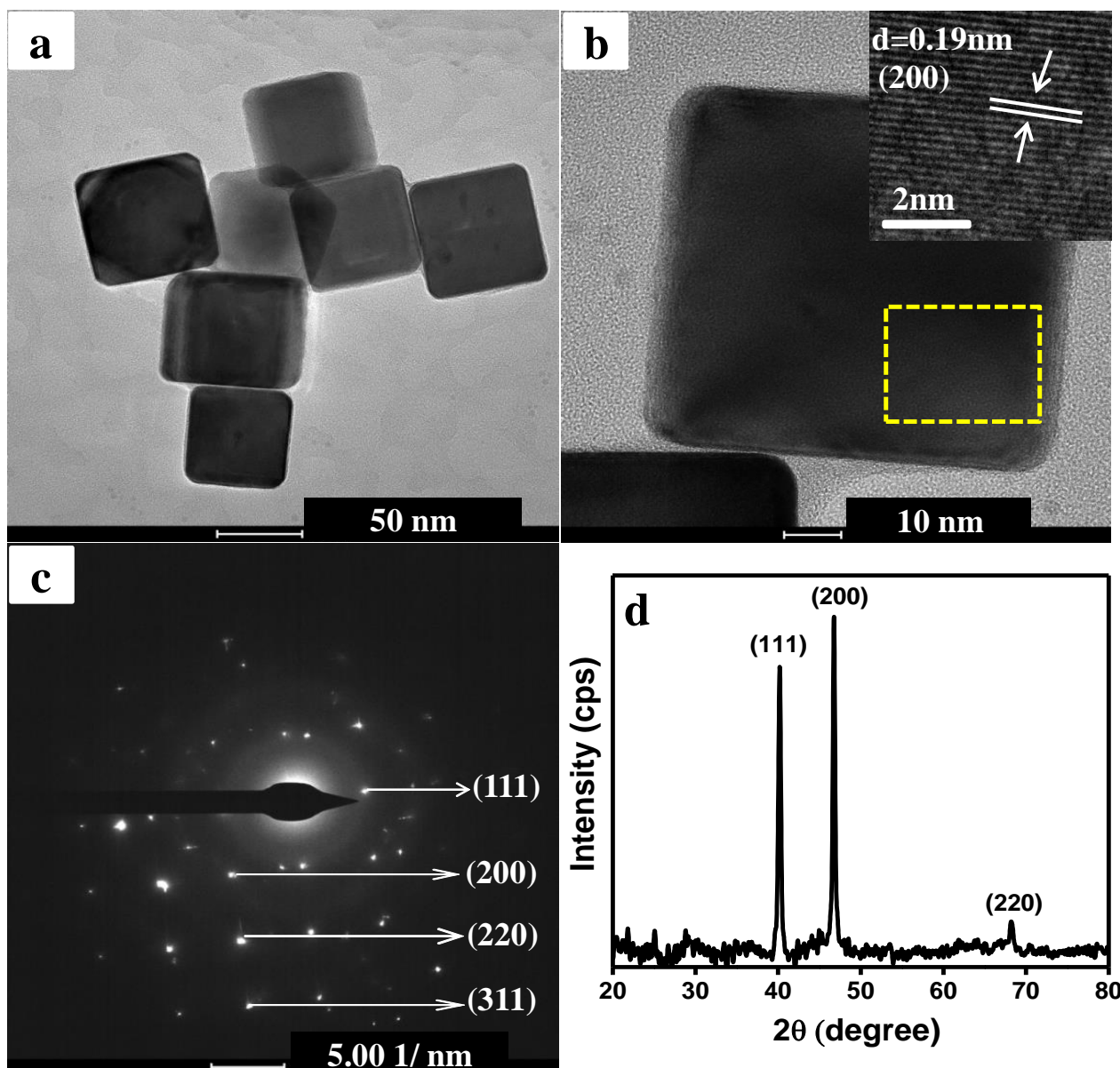


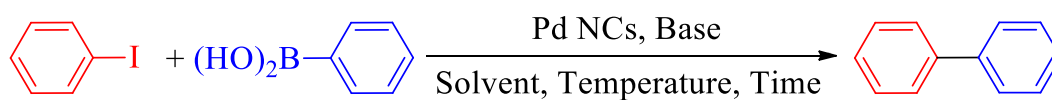
**Figure 4.** (a) TEM image of Pd NCs, (b) HRTEM image of the selected square corner of an individual Pd NCs having  $d$  spacing 0.19 nm corresponds to (200) lattice plane of Pd NCs. (c) SAED pattern of Pd NCs and (d) XRD pattern of Pd NCs.

Transmission electron microscopy (TEM) images were in well agreement with the morphologies observed in FESEM. Fig. 4(a) shows the TEM image of monodisperse Pd NCs. The high resolution TEM image mentioned in Fig. 4(b) clearly shows lattice fringes with a measured  $d$ -spacing of 0.19 nm corresponds to (200) plane of Pd. The selected area electron diffraction (SAED) pattern in Fig. 4(c) shows the Debye-Scherrer rings of Pd NCs corresponds to (111), (200), (220) and (311) reflection planes of the Pd nanocrystal.<sup>6</sup> The SAED pattern is suitably supported by the powder X-ray diffraction (PXRD) and confirmed the crystalline lattice structure of the Pd NCs. The diffraction

1  
2  
3 pattern of the Pd NCs is shown in the Fig. 4(d). The spacing value  $d = 0.19$  nm was calculated on  
4 the basis of Bragg's law following the formula  $n \lambda = 2d \sin\theta$ . The diffraction peaks at  $2\theta$  values  
5 obtained are  $40.09^\circ$ ,  $46.57^\circ$  and  $68.87^\circ$  corresponds to the (111), (200) and (220) crystal planes of  
6 Pd NCs, respectively. The sharp intense peak of the above-mentioned planes confirms the  
7 crystalline nature of the Pd NCs. The diffraction planes of Pd NCs are well matches with the JCPDS  
8 (file no. 87-0638) and face centered cubic (fcc) arrangements.  
9  
10  
11  
12  
13  
14

### 15 Application of the Pd NCs in Suzuki-Miyaura cross-coupling reactions

16 The Suzuki-Miyaura cross-coupling is a simple and reliable organic transformation for the synthesis  
17 of C-C cross-coupled products. The ability to tolerate a wide range of functional groups, mild  
18 reaction conditions and easily available reagents are some of the key advantages of employing  
19 Suzuki-Miyaura cross-coupling reaction. Thus, following the successful characterization of Pd NCs  
20 by various analytical techniques, we have proceeded with the catalytic activity study in Suzuki-  
21 Miyaura cross-coupling reaction. The cross-coupling between iodobenzene and phenylboronic acid  
22 was chosen as the model reaction for optimization of the reaction conditions (Scheme 1). Following  
23 a series of reactions by altering various parameters, the Suzuki-Miyaura cross-coupling reaction  
24 was optimized as shown in Table 1.  
25  
26  
27  
28  
29  
30  
31



**Scheme 1.** Suzuki–Miyaura cross-coupling reaction of iodobenzene with phenylboronic acid.

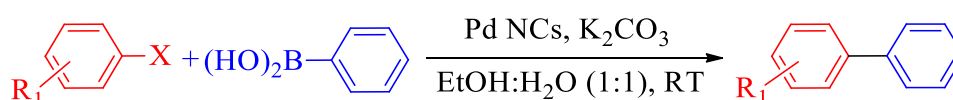
Among the bases used,  $K_2CO_3$  (Table 1, entry 2) was found to be effective when compared with other bases like  $Na_2CO_3$  (Table 1, entry 3),  $NaOH$  (Table 1, entry 4) and  $KOH$  (Table 1, entry 5). In case of solvent system,  $H_2O:EtOH$  (1:1) system was found to be superior (Table 1, entry 2). When only  $EtOH$  (Table 1, entry 7) and  $MeOH$  (Table 1, entry 7) were used, the yields obtained were not appreciable. Also, there was no improvement in the yield when acetonitrile (ACN) (Table 1, entry 8) or toluene (Table 1, entry 10) was employed. The optimum reaction temperature was found to be room temperature (Table 1, entry 2) since there was no any improvement in the yield with increase in temperatures (Table 1, entries 11-13)

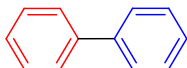
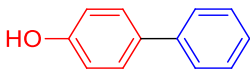
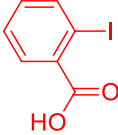
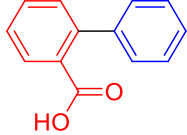
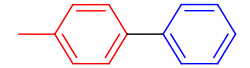
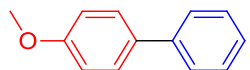
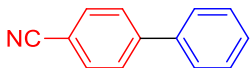
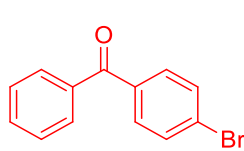
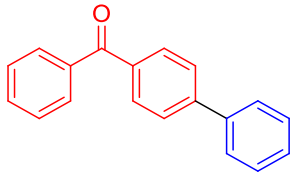
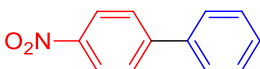
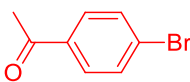
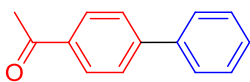
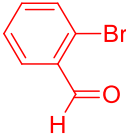
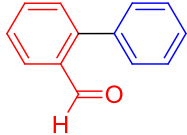
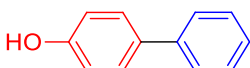
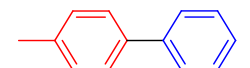
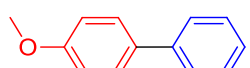
**Table 1.** Optimization of reaction conditions for model Suzuki-Miyaura cross-coupling reaction in the presence of Pd NCs<sup>a</sup>

Entry	Base	Solvent	Temp. (°C)	Catalyst (mg)	Time (h)	Yield (%) <sup>b</sup>
1	K <sub>2</sub> CO <sub>3</sub>	H <sub>2</sub> O:EtOH(1:1)	R.T	4	0.5	95
<b>2</b>	<b>K<sub>2</sub>CO<sub>3</sub></b>	<b>H<sub>2</sub>O:EtOH(1:1)</b>	<b>R.T</b>	<b>2</b>	<b>0.5</b>	<b>95</b>
3	Na <sub>2</sub> CO <sub>3</sub>	H <sub>2</sub> O:EtOH(1:1)	R.T	2	0.67	90
4	NaOH	H <sub>2</sub> O:EtOH(1:1)	R.T	2	0.5	80
5	KOH	H <sub>2</sub> O:EtOH(1:1)	R.T	2	0.67	70
6	K <sub>2</sub> CO <sub>3</sub>	H <sub>2</sub> O	R.T	2	0.67	80
7	K <sub>2</sub> CO <sub>3</sub>	EtOH	R.T	2	0.5	75
8	K <sub>2</sub> CO <sub>3</sub>	ACN	R.T	2	1	75
9	K <sub>2</sub> CO <sub>3</sub>	MeOH	R.T	2	1	72
10	K <sub>2</sub> CO <sub>3</sub>	Toluene	R.T	2	1	80
11	K <sub>2</sub> CO <sub>3</sub>	H <sub>2</sub> O:EtOH(1:1)	40	2	0.5	95
12	K <sub>2</sub> CO <sub>3</sub>	H <sub>2</sub> O:EtOH(1:1)	50	2	0.5	95
13	K <sub>2</sub> CO <sub>3</sub>	H <sub>2</sub> O:EtOH(1:1)	60	2	0.5	95
14	K <sub>2</sub> CO <sub>3</sub>	H <sub>2</sub> O:EtOH(1:1)	R.T	3	0.5	95
15	K <sub>2</sub> CO <sub>3</sub>	H <sub>2</sub> O:EtOH(1:1)	R.T	1	0.5	90
16	K <sub>2</sub> CO <sub>3</sub>	H <sub>2</sub> O:EtOH(1:1)	R.T	1	1	90
17	K <sub>2</sub> CO <sub>3</sub>	H <sub>2</sub> O:EtOH(1:1)	R.T	2	1	95
18	K <sub>2</sub> CO <sub>3</sub>	H <sub>2</sub> O:EtOH(1:1)	R.T	2	0.25	90

<sup>a</sup>Reaction conditions: iodobenzene (0.27 mmol), phenylboronic acid (0.30 mmol), base (0.60 mmol) and solvent (5 mL) in air. <sup>b</sup>Isolated yield after separation by column chromatography.

**Table 2.** Suzuki-Miyaura cross-coupling reactions of different aryl halides with phenylboronic acid catalyzed by Pd NCs<sup>a</sup>



Entry	Aryl halide	Product	Time (h)	Yield (%) <sup>b</sup>	TON
01			0.5	95	1242
02			0.5	92	1115
03			0.5	90	968
04			0.5	93	1137
05			0.5	92	1048
06			0.5	90	1319
07 <sup>c</sup>			1	85	868
08			0.5	91	1201
09 <sup>c</sup>			2	82	1099
10 <sup>c</sup>			2	80	1153
11			1	92	1563
12 <sup>c</sup>			2	88	1356
13 <sup>c</sup>			1	86	1341
14 <sup>c</sup>			1	88	1255

<sup>a</sup>Reaction conditions: aryl halide (0.27 mmol), phenylboronic acid (0.30 mmol), Pd NCs (2 mg), base (0.60 mmol) and EtOH: H<sub>2</sub>O (1:1) (5 mL) in air. <sup>b</sup>Isolated yield after separation by column chromatography. <sup>c</sup>Reaction carried out at 50 °C.

The cross-coupling yield increased with increase in the catalyst ratio from 1 mg to 2 mg (Table 1, entries 15 and 2). But further increase in the catalyst quantity (Table 1, entries 1 and 14) does not have any effect in the yield and hence 2 mg of the catalyst was found to be most favourable Pd NC ratio (Table 1, entry 2). Increase in the reaction time from 0.25 h (Table 1, entry 18) to 0.5 h (Table 1, entry 2) increased the yield but further increase in time to 1 h (Table 1, entry 17) does not increase the yield and hence 0.5 h was finalized to be the optimum time duration for the Suzuki-Miyaura cross-coupling with Pd NCs. After optimizing the reaction conditions, the scope of Pd NCs was studied for various aryl halides to understand the general applicability of the catalyst which is represented in Table 2. From the results obtained it can be generalized that Pd NCs are highly active and could catalyse the cross-coupling reaction very efficiently for aryl halides with different electron withdrawing as well as electron donating groups to give good to excellent yields. Also, aryl iodides were faster to react when compared with their bromide counterparts. In addition, external heating was required in most of the cases for aryl bromides to undergo cross-coupling with phenylboronic acid.

**Table 3.** Comparison of results for Pd NCs catalyst with other Pd catalysts for Suzuki–Miyaura cross-coupling reaction between iodobenzene and phenylboronic acid.

Entry	Catalyst	Solvent	Temp. (°C)	Time (h)	Yield (%)	Ref.
1	Pd NRs	EtOH:H <sub>2</sub> O (4:1)	85	4	92	6
2	Pd Nanoclusters	NMP:H <sub>2</sub> O	100	5	89	52
3	Pd NPs	CH <sub>3</sub> OH:CH <sub>3</sub> CN (1:1)	R.T	2	99	53
4	Pd-acac-am- Fe <sub>3</sub> O <sub>4</sub> @SiO <sub>2</sub>	DMF:H <sub>2</sub> O (8:2)	80	2	98	54
5	Pd NPs@CS	EtOH:H <sub>2</sub> O (1:1)	65	3	98	55
6	Pd/AIO(OH) NPs	IPA:H <sub>2</sub> O (1:1)	R.T	2	98	56
7	MUA-Pd	DMF	90	8	99	57
8	C/Co@PNIPAM	Toluene:H <sub>2</sub> O (2:1)	85	16	99	58
9	Pd(II)-NiFe <sub>2</sub> O <sub>4</sub>	EtOH:H <sub>2</sub> O (9:1)	80	3	96	59
<b>10</b>	<b>Pd NCs</b>	<b>EtOH:H<sub>2</sub>O (1:1)</b>	<b>R.T</b>	<b>0.5</b>	<b>95</b>	<b>Present work</b>

In order to understand the exceptionality and unique activity of the synthesized Pd NCs, the catalytic properties of synthesized catalyst was compared with other reports towards C-C cross coupling reactions between substituted aryl iodide/bromide with phenylboronic acid. The results of Suzuki-Miyaura cross-coupling shows a better catalytic activity with high yield in shorter reaction time and milder reaction conditions for Pd NCs catalyst compared to other Pd NPs supported on different supports as shown in Table 3.

### Recyclability of the Pd NCs in Suzuki-Miyaura cross-coupling reactions

Recyclability is a vital factor which assesses the greenness and the sustainability of every catalyst in any organic transformation. Hence, Pd NCs were subjected to recyclability study on the model of Suzuki-Miyaura cross-coupling reaction and the results obtained are depicted in Fig. 5.

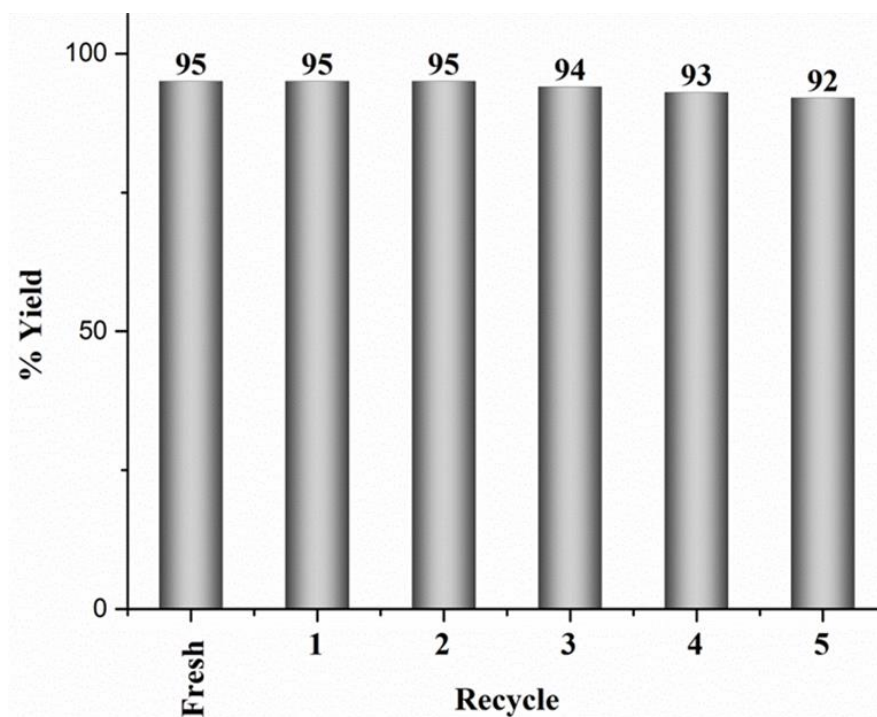


**Figure 5.** The recycling efficiency of Pd NCs in Suzuki-Miyaura cross-coupling reaction.

The results obtained from it can be understood that there is no significant change in the catalytic activity of Pd NCs with the yield reaching up to 92 % from 95 % by the end of fifth recycle. The Pd NCs characterized by FESEM given in Figure S4 after the fifth recycle of Suzuki-Miyaura cross-coupling shows that there is slight characteristic change in the morphology of Pd NCs.

## Reduction of *p*-NP

The catalytic reduction of *p*-NP to *p*-AP was initially evaluated by the addition of pale-yellow coloured aqueous solution of *p*-NP which exhibits a characteristic absorption peak at 317 nm. The addition of NaBH<sub>4</sub> to *p*-NP, colour of the solution changes to dark yellow and shows a characteristic peak at 400 nm due to the formation of phenolate ion as shown in Fig. 6 (a). In order to understand the role of catalyst, the reaction proceeded up to 1h without the addition of Pd NCs as shown in Fig. 6 (b). Interestingly, it has seen that the reduction of nitro-group did not proceed in the absence of catalyst because the kinetic barrier between the two negative ions of *p*-NP and BH<sub>4</sub><sup>-</sup> is extremely high and NaBH<sub>4</sub> is not able to overcome the barrier alone.<sup>49</sup> However, the addition of Pd NCs a new absorption band appeared at 313 nm with the simultaneous decrease in the absorption peak of phenolate ion and peak for *p*-NP at 317 nm vanishes completely.

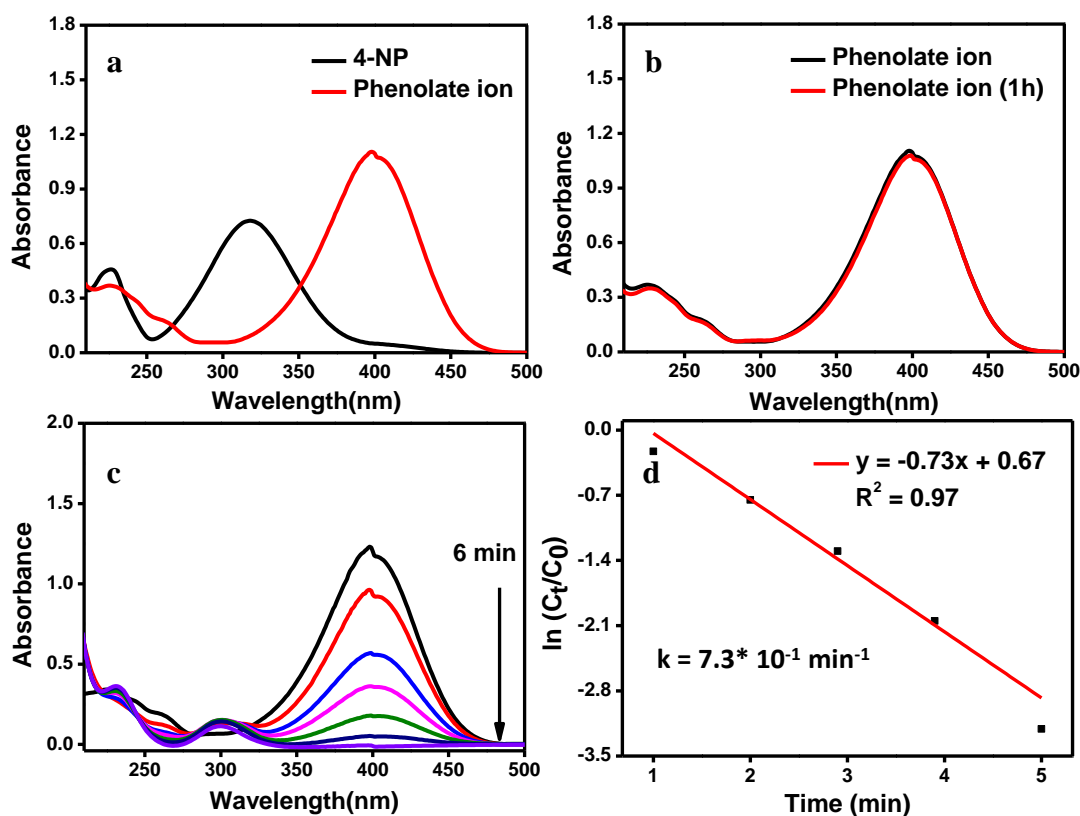


**Figure 6.** (a) Absorption peaks at 317 and 400 nm represents the characteristic peak for *p*-NP and phenolate ions, respectively, (b) represents the progress of reaction without addition of catalyst, (c) successive reduction of *p*-NP to *p*-AP with 70 μL Pd NCs catalyst and (d) kinetic plot of  $\ln(C_t/C_0)$  vs time for the reduction of *p*-NP.

In order to study the doses of catalyst, primarily 1 mg/mL of catalyst concentration was prepared. It was seen that even after the addition of 100 μL of catalyst the reduction proceeded slowly, with

rate constant,  $k = 0.4 \times 10^{-1} \text{ min}^{-1}$  and 85 % conversion obtained after 40 min of reaction shown in Fig. S5. Hence, the catalyst concentration was increased. Initially, different volumes of 10, 30, 50 and 70  $\mu\text{L}$  Pd NCs catalyst of concentration 2 mg/mL were added and allowed to perform the reduction. It was seen that 70  $\mu\text{L}$  of Pd NCs performed maximum conversion up to 99 % in 6 min as shown in Fig. 6 (c). The comparison of different loading of the catalyst shown in Fig. S6 and Table S1 shows the variations of rate of the reaction, time and conversion % with stepwise increase in the catalyst amount. The colour changes from light yellow to dark yellow due to the addition of  $\text{NaBH}_4$  gives the information about the alkalinity of the solution and a colourless solution was observed after reduction on the surface of catalyst is shown in Figure S7. The pathway of catalysed reduction reaction follows first order kinetics which has confirmed through the linear correlation curve obtained from the plot  $\ln(C_t/C_0)$  versus time based on the absorbance. The rate constant,  $k$  was calculated and found to be  $7.3 \times 10^{-1} \text{ min}^{-1}$  for 70  $\mu\text{L}$  of Pd NCs whereas for 10, 30 and 50  $\mu\text{L}$ , the rate constant was observed  $10^{-2}$ ,  $2.4 \times 10^{-1}$  and  $3.8 \times 10^{-1} \text{ min}^{-1}$ , respectively.

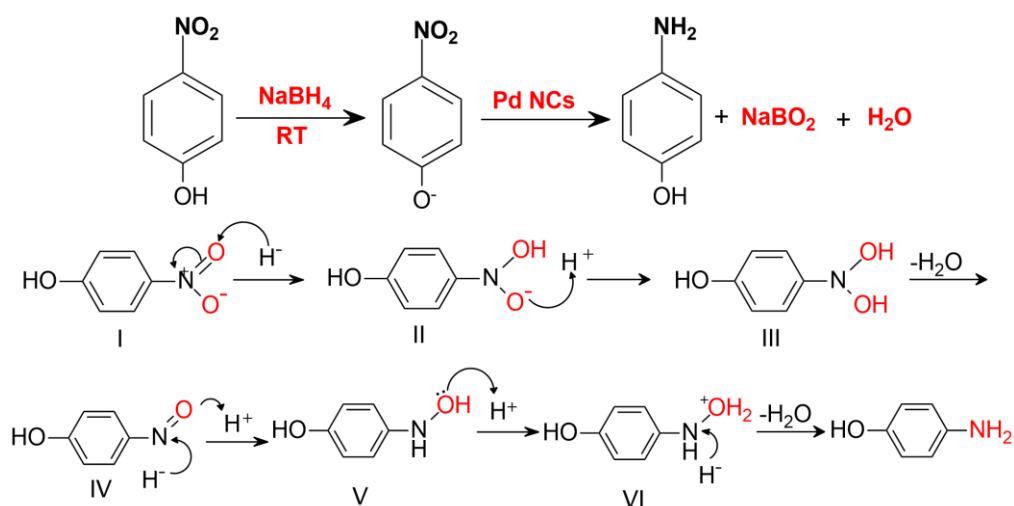


**Figure 7.** Steps involved in the reduction of *p*-NP to *p*-AP using Pd NCs as catalyst,  $\text{NaBH}_4$  as hydrogen source under RT using aqueous solvent.

The progress of the reduction reaction described as, adsorption of both the donor  $\text{BH}_4^-$  and acceptor *p*-NP molecules to the catalytic surface which led electron transfer from donor to acceptor and provide the reduction product, *p*-AP. Addition of  $\text{NaBH}_4$  to the reactant leads the formation of phenolate ion which retain its position in absence of catalyst. Whereas subsequently addition of catalyst, leads transformation of hydride from  $\text{BH}_4^-$  to the reactant. Fig. 7 represents the stepwise plausible reduction mechanism from *p*-NP to *p*-AP using Pd NCs as a catalyst to overcome

activation energy barrier of two repelling negatively charged anions.<sup>60</sup> Comparison of the literature results are summarized in Table 4 for the hydrogenation of *p*-NP using various Pd nanocatalyst, which concern the importance of anisotropic Pd NCs catalyst towards the reaction.

**Table 4.** Comparison of Pd Nanocatalyst used in *p*-NP reduction reaction.

Entry	Catalyst	Time (min)	k (min <sup>-1</sup> )	Ref.
1	Pd/MPC	7	1.2*10 <sup>-2</sup>	49
2	Pd-graphene nanohybrid	12	1.4*10 <sup>-1</sup>	61
3	PdNPs stabilized in XG	24	1.84.1*10 <sup>-1</sup>	62
4	UiO-66-NH <sub>2</sub> @COP@Pd	7	3.1*10 <sup>-1</sup>	63
5	Pd NP/CNT	7	6.32*10 <sup>-1</sup>	64
<b>6</b>	<b>Pd NCs</b>	<b>6</b>	<b>7.3*10<sup>-1</sup></b>	<b>Present work</b>

## Conclusion

Anisotropic monodisperse Pd NCs were synthesized using seed mediated wet chemical synthesis in two step process. Smaller cubic Pd seeds were synthesized for the growth of Pd NCs of sharp edges with high yield. The synthesized Pd NCs shows well-defined morphology throughout the sample. Spectroscopic and microscopic tools were used for the characterization of the synthesized Pd NCs. These Pd NCs were found to perform highly efficient heterogeneous catalyst for Suzuki-Miyaura cross coupling reaction as well as for *p*-NP reduction. It exhibited enhanced activity, greater selectivity and stability of the Pd NCs. The recyclability study of Pd NCs showed a high catalytic activity even after performing five consecutive cycles. The better catalytic activity of Pd NCs can be attributed to its increase in surface energy associated with the different planes of the nanocubes or increase in coordination atom on the low index crystallographic facets sites which help them to act as the surface-active agent. These catalysts may attract useful attention for further applications.

## Associated Content

### Supporting Information

The Supporting Information is available free of charge at <http://pubs.acs.org/doi/xxxxxx>

EDS spectrum, DLS measurement, Zeta potential measurement, FESEM images of Pd NCs and  $^1\text{H}$  NMR spectra of cross-coupled products.

### Author Contributions

The manuscript was written through contributions of all authors. All authors have given approval to the final version of the manuscript.

† These authors contributed equally.

### Acknowledgements

BMB acknowledges JAIN University for junior research fellowship. S.S and AKS are grateful to the SERB, New Delhi, India for funding to conduct the research (CRG/2018/003533). The authors thankful to Nano Mission (SR/NM/NS-20/2014) for FESEM facility at Jain University.

### Notes

The authors declare no conflict of interest.

### References

- (1) Burrows, N. D.; Vartanian, A. M.; Abadeer, N. S.; Grzincic, E. M.; Jacob, L. M.; Lin, W.; Li, J.; Dennison, J. M.; Hinman, J. G.; Murphy, C. J., Anisotropic nanoparticles and anisotropic surface chemistry. *J. Phys. Chem. Lett.* **2016**, 7(4), 632-641. <https://doi.org/10.1021/acs.jpcclett.5b02205>.
- (2) Link, S.; El-Sayed, M. A., Spectral properties and relaxation dynamics of surface plasmon electronic oscillations in gold and silver nanodots and nanorods. *J. Phys. Chem.* **1999**, 103 8410-8426. <https://doi.org/10.1021/jp9917648>.
- (3) Zhang, Y.; Grass, M. E.; Kuhn, J. N.; Tao, F.; Habas, S. E.; Huang, W.; Yang, P.; Somorjai, G. A., Highly selective synthesis of catalytically active monodisperse rhodium nanocubes. *J. Am. Chem. Soc.* **2008**, 130 (18), 5868-5869. <https://doi.org/10.1021/ja801210s>.
- (4) Zhang, H.; Jin, M.; Xiong, Y.; Lim, B.; Xia, Y., Shape-controlled synthesis of Pd nanocrystals and their catalytic applications. *Acc. Chem. Res.* **2013**, 46 (8), 1783-1794. <https://doi.org/10.1021/ar300209w>.
- (5) Huang, X.; Tang, S.; Zhang, H.; Zhou, Z.; Zheng, N., Controlled formation of concave tetrahedral/trigonal bipyramidal palladium nanocrystals. *J. Am. Chem. Soc.* **2009**, 131 (39), 13916-13917. <https://doi.org/10.1021/ja9059409>.
- (6) Chen, Y.-H.; Hung, H.-H.; Huang, M. H., Seed-mediated synthesis of palladium nanorods and branched nanocrystals and their use as recyclable Suzuki coupling reaction catalysts. *J. Am. Chem. Soc.* **2009**, 131 (25), 9114-9121. <https://doi.org/10.1021/ja903305d>.

- 1  
2  
3 (7) Lim, B.; Jiang, M.; Tao, J.; Camargo, P. H.; Zhu, Y.; Xia, Y., Shape-controlled synthesis of Pd  
4 nanocrystals in aqueous solutions. *Adv. Funct. Mater.* **2009**, *19* (2), 189-200.  
5 <https://doi.org/10.1002/adfm.200801439>.  
6  
7  
8 (8) Xiong, Y.; Cai, H.; Yin, Y.; Xia, Y., Synthesis and characterization of fivefold twinned nanorods  
9 and right bipyramids of palladium. *Chem. Phys. Lett.* **2007**, *440* (4-6), 273-278.  
10 <https://doi.org/10.1016/j.cplett.2007.04.074>.  
11  
12  
13 (9) Antolini, E., Palladium in fuel cell catalysis. *Energy Environ. Sci.* **2009**, *2* (9), 915-931.  
14 <https://doi.10.1039/B820837A>.  
15  
16  
17 (10) Sawoo, S.; Srimani, D.; Dutta, P.; Lahiri, R.; Sarkar, A., Size controlled synthesis of Pd  
18 nanoparticles in water and their catalytic application in C–C coupling reactions. *Tetrahedron* **2009**,  
19 *65* (22), 4367-4374. <https://doi.org/10.1016/j.tet.2009.03.062>.  
20  
21  
22 (11) Zhou, W.; Zhou, Z.; Song, S.; Li, W.; Sun, G.; Tsiakaras, P.; Xin, Q., Pt based anode catalysts for  
23 direct ethanol fuel cells. *Appl. Catal. B* **2003**, *46* (2), 273-285. [https://doi.org/10.1016/S0926-](https://doi.org/10.1016/S0926-3373(03)00218-2)  
24 [3373\(03\)00218-2](https://doi.org/10.1016/S0926-3373(03)00218-2).  
25  
26  
27 (12) Nørskov, J. K.; Rossmeisl, J.; Logadottir, A.; Lindqvist, L.; Kitchin, J. R.; Bligaard, T.; Jonsson,  
28 H., Origin of the overpotential for oxygen reduction at a fuel-cell cathode. *J. Phys. Chem. B* **2004**,  
29 *108* (46), 17886-17892. <https://doi.org/10.1021/jp047349j>.  
30  
31  
32 (13) Strasser, P.; Fan, Q.; Devenney, M.; Weinberg, W. H.; Liu, P.; Nørskov, J. K., High throughput  
33 experimental and theoretical predictive screening of materials– a comparative study of search  
34 strategies for new fuel cell anode catalysts. *J. Phys. Chem. B* **2003**, *107* (40), 11013-11021.  
35 <https://doi.org/10.1021/jp030508z>.  
36  
37  
38  
39 (14) Lamy, C.; Rousseau, S.; Belgsir, E.; Coutanceau, C.; Léger, J.-M., Recent progress in the direct  
40 ethanol fuel cell: development of new platinum–tin electrocatalysts. *Electrochim. Acta* **2004**, *49*  
41 (22-23), 3901-3908. <https://doi.org/10.1016/j.electacta.2004.01.078>.  
42  
43  
44 (15) Li, H.; Xin, Q.; Li, W.; Zhou, Z.; Jiang, L.; Yang, S.; Sun, G., An improved palladium-based  
45 DMFCs cathode catalyst. *Chem. Commun.* **2004**, *23*, 2776-2777. <https://doi.org/10.1039/B409539A>.  
46  
47  
48 (16) Lopes, T.; Antolini, E.; Gonzalez, E., Carbon supported Pt–Pd alloy as an ethanol tolerant oxygen  
49 reduction electrocatalyst for direct ethanol fuel cells. *Int. J. Hydrogen Energy* **2008**, *33* (20), 5563-  
50 5570. <https://doi.org/10.1016/j.ijhydene.2008.05.030>.  
51  
52  
53 (17) Yin, L.; Liebscher, J., Carbon– carbon coupling reactions catalyzed by heterogeneous palladium  
54 catalysts. *Chem. Rev.* **2007**, *107* (1), 133-173. [doi.org/10.1021/cr0505674](https://doi.org/10.1021/cr0505674).  
55  
56  
57 (18) Scarabelli, L.; Coronado-Puchau, M.; Giner-Casares, J. J.; Langer, J.; Liz-Marzán, L. M.,  
58 Monodisperse gold nanotriangles: size control, large-scale self-assembly, and performance in  
59  
60

- 1  
2  
3 surface-enhanced Raman scattering. *ACS Nano* **2014**, *8* (6), 5833-5842.  
4 <https://doi.org/10.1021/nn500727w>.  
5
- 6 (19) Tebbe, M.; Maennel, M.; Fery, A.; Pazos-Perez, N.; Alvarez-Puebla, R. A., Organized solid thin  
7 films of gold nanorods with different sizes for surface-enhanced Raman scattering applications. *J.*  
8 *Phys. Chem. C* **2014**, *118* (48), 28095-28100. <https://doi.org/10.1021/jp5086685>.  
9
- 10 (20) Li, J. F.; Huang, Y. F.; Ding, Y.; Yang, Z. L.; Li, S. B.; Zhou, X. S.; Fan, F. R.; Zhang, W.; Zhou,  
11 Z. Y.; Ren, B., Shell-isolated nanoparticle-enhanced Raman spectroscopy. *Nature* **2010**, *464* (7287),  
12 392-395. <https://doi.org/10.1038/nature08907>.  
13
- 14 (21) a) Tian, Z.-Q.; Ren, B., Adsorption and reaction at electrochemical interfaces as probed by surface-  
15 enhanced Raman spectroscopy. *Annu. Rev. Phys. Chem.* **2004**, *55*, 197-229. b) Tian, Z.-Q.; Ren, B.;  
16 Li, J.-F.; Yang, Z.-L., Expanding generality of surface-enhanced Raman spectroscopy with  
17 borrowing SERS activity strategy. *Chem. Commun.* **2007**, (34), 3514-3534.  
18 <https://doi.org/10.1039/B616986D>.  
19
- 20 (22) Balanta, A.; Godard, C.; Claver, C., Pd nanoparticles for C–C coupling reactions. *Chem. Soc. Rev.*  
21 **2011**, *40* (10), 4973-4985. <https://doi.org/10.1039/C1CS15195A>.  
22
- 23 (23) Fihri, A.; Bouhrara, M.; Nekoueishahraki, B.; Basset, J.-M.; Polshettiwar, V., Nanocatalysts for  
24 Suzuki cross-coupling reactions. *Chem. Soc. Rev.* **2011**, *40* (10), 5181-5203.  
25 <https://doi.org/10.1039/C1CS15079K>.  
26
- 27 (24) Sonogashira, K.; Negishi, E.; de Meijere, A., Handbook of Organopalladium Chemistry for Organic  
28 Synthesis Wiley. Interscience, New York: **2002**, 1, 1123-1662.  
29
- 30 (25) Diederich, F.; Stang, P. J., Metal-catalyzed cross-coupling reactions. John Wiley & Sons: **2008**.  
31
- 32 (26) Reetz, M. T.; Westermann, E., Phosphane-free palladium-catalyzed coupling reactions: the decisive  
33 role of Pd nanoparticles. *Angew. Chem., Int. Ed.* **2000**, *39* (1), 165-168.  
34 [https://doi.org/10.1002/\(SICI\)1521-3773\(20000103\)39:1<165::AID-ANIE165>3.0.CO;2-B](https://doi.org/10.1002/(SICI)1521-3773(20000103)39:1<165::AID-ANIE165>3.0.CO;2-B)  
35
- 36 (27) Li, Y.; Hong, X. M.; Collard, D. M.; El-Sayed, M. A., Suzuki cross-coupling reactions catalyzed  
37 by palladium nanoparticles in aqueous solution. *Org. Lett.* **2000**, *2* (15), 2385-2388.  
38 <https://doi.org/10.1021/ol0061687>.  
39
- 40 (28) Kim, S.-W.; Kim, M.; Lee, W. Y.; Hyeon, T., Fabrication of hollow palladium spheres and their  
41 successful application to the recyclable heterogeneous catalyst for Suzuki coupling reactions. *J. Am.*  
42 *Chem. Soc.* **2002**, *124* (26), 7642-7643. <https://doi.org/10.1021/ja026032z>.  
43
- 44 (29) Lim, B.; Jiang, M.; Tao, J.; Camargo, P. H.; Zhu, Y.; Xia, Y., Shape-controlled synthesis of Pd  
45 nanocrystals in aqueous solutions. *Adv. Funct. Mater.* **2009**, *19* (2), 189-200.  
46 <https://doi.org/10.1002/adfm.200801439>.  
47  
48  
49  
50  
51  
52  
53  
54  
55  
56  
57  
58  
59  
60

- 1  
2  
3 (30) Yuan, B.; Pan, Y.; Li, Y.; Yin, B.; Jiang, H., A highly active heterogeneous palladium catalyst for  
4 the Suzuki–Miyaura and Ullmann coupling reactions of aryl chlorides in aqueous media. *Angew.*  
5 *Chem. Int. Ed.* **2010**, *49* (24), 4054-4058. <https://doi.org/10.1002/anie.201000576>.  
6  
7  
8 (31) Khairul, W. M.; Mei, M.; Rahamathullah, R.; Soh, S. K. C.; Shamsuddin, M. In Palladium (II)  
9 Picoline Thiourea Complex as Homogenous Catalyst in Heck Cross-Coupling Reaction in the  
10 Formation of C=C Bond, Solid State Phenomena, *Trans Tech Publ.* **2018**, 115-121.  
11 <https://doi.org/10.4028/www.scientific.net/SSP.273.115>.  
12  
13 (32) Jia, X.; Jiang, D.; Tsang, D. C.; Choi, J.; Yip, A. C., Stacking MFI zeolite structures for improved  
14 Sonogashira coupling reactions. *Microporous and Mesoporous Materials* **2019**, *276*, 147-153.  
15 <https://doi.org/10.1016/j.micromeso.2018.09.039>.  
16  
17 (33) Liu, Y.; Bai, X.; Li, S., In-situ preparation of Pd nanoparticles in the pore channel of CMK-3 for  
18 Suzuki coupling reaction. *Microporous and Mesoporous Materials* **2018**, *260*, 40-44.  
19 <https://doi.org/10.1016/j.micromeso.2017.06.006>.  
20  
21 (34) Pérez-Lorenzo, M., Palladium nanoparticles as efficient catalysts for Suzuki cross-coupling  
22 reactions. *J. Phys. Chem. Lett.* **2012**, *3* (2), 167-174. <https://doi.org/10.1021/jz2013984>.  
23  
24 (35) Kandathil, V.; Koley, T. S.; Manjunatha, K.; Dateer, R. B.; Keri, R. S.; Sasidhar, B.; Patil, S. A.;  
25 Patil, S. A., A new magnetically recyclable heterogeneous palladium (II) as a green catalyst for  
26 Suzuki-Miyaura cross-coupling and reduction of nitroarenes in aqueous medium at room  
27 temperature. *Inorg. Chim. Acta* **2018**, *478*, 195-210. <https://doi.org/10.1016/j.ica.2018.04.015>.  
28  
29 (36) Manjunatha, K.; Koley, T. S.; Kandathil, V.; Dateer, R. B.; Balakrishna, G.; Sasidhar, B.; Patil, S.  
30 A.; Patil, S. A., Magnetic nanoparticle-tethered Schiff base–palladium (II): Highly active and  
31 reusable heterogeneous catalyst for Suzuki–Miyaura cross-coupling and reduction of nitroarenes in  
32 aqueous medium at room temperature. *Appl. Organomet. Chem.* **2018**, *32* (4), e4266.  
33 <https://doi.org/10.1002/aoc.4266>.  
34  
35 (37) Vishal, K.; Fahlman, B. D.; Sasidhar, B.; Patil, S. A.; Patil, S. A., Magnetic nanoparticle-supported  
36 N-heterocyclic carbene-palladium (II): A convenient, efficient and recyclable catalyst for Suzuki–  
37 Miyaura cross-coupling reactions. *Catal. Lett.* **2017**, *147* (4), 900-918.  
38 <https://doi.org/10.1007/s10562-017-1987-7>.  
39  
40 (38) Kempasiddhaiah, M.; Kandathil, V.; Dateer, R. B.; Sasidhar, B. S.; Patil, S. A.; Patil, S. A.,  
41 Magnetite tethered mesoionic carbene-palladium (II): An efficient and reusable nanomagnetic  
42 catalyst for Suzuki-Miyaura and Mizoroki-Heck cross-coupling reactions in aqueous medium. *Appl.*  
43 *Organomet. Chem.* **2019**, *33* (5), e4846. <https://doi.org/10.1002/aoc.4846>.  
44  
45  
46  
47  
48  
49  
50  
51  
52  
53  
54  
55  
56  
57  
58  
59  
60

- 1  
2  
3 (39) Pandey, S.; Mishra, S. B., Catalytic reduction of p-nitrophenol by using platinum nanoparticles  
4 stabilised by guar gum. *Carbohydr. Polym.* **2014**, *113*, 525-531.  
5 <https://doi.org/10.1016/j.carbpol.2014.07.047>.  
6  
7  
8 (40) Marais, E.; Nyokong, T., Adsorption of 4-nitrophenol onto Amberlite® IRA-900 modified with  
9 metallophthalocyanines. *J. Hazard. Mater.* **2008**, *152* (1), 293-301.  
10 <https://doi.org/10.1016/j.jhazmat.2007.06.096>.  
11  
12  
13 (41) O'Connor, O. A.; Young, L., Toxicity and anaerobic biodegradability of substituted phenols under  
14 methanogenic conditions. *Environ. Toxicol. Chem.* **1989**, *8* (10), 853-862.  
15 <https://doi.org/10.1002/etc.5620081003>.  
16  
17  
18 (42) Dieckmann, M. S.; Gray, K. A., A comparison of the degradation of 4-nitrophenol via direct and  
19 sensitized photocatalysis in TiO<sub>2</sub> slurries. *Water Res.* **1996**, *30* (5), 1169-1183.  
20 [https://doi.org/10.1016/0043-1354\(95\)00240-5](https://doi.org/10.1016/0043-1354(95)00240-5).  
21  
22  
23 (43) Modirshahla, N.; Behnajady, M.; Mohammadi-Aghdam, S., Investigation of the effect of different  
24 electrodes and their connections on the removal efficiency of 4-nitrophenol from aqueous solution  
25 by electrocoagulation. *J. Hazard. Mater.* **2008**, *154* (1-3), 778-786. [https://doi.org/10.1016/0043-](https://doi.org/10.1016/0043-1354(95)00240-5)  
26 [1354\(95\)00240-5](https://doi.org/10.1016/0043-1354(95)00240-5).  
27  
28  
29  
30 (44) Esumi, K.; Isono, R.; Yoshimura, T., Preparation of PAMAM- and PPI- metal (silver, platinum,  
31 and palladium) nanocomposites and their catalytic activities for reduction of 4-nitrophenol.  
32 *Langmuir* **2004**, *20* (1), 237-243. <https://doi.org/10.1021/la035440t>.  
33  
34  
35 (45) Shin, K. S.; Choi, J.-Y.; Park, C. S.; Jang, H. J.; Kim, K., Facile synthesis and catalytic application  
36 of silver-deposited magnetic nanoparticles. *Catal. Lett.* **2009**, *133* (1-2), 1-7.  
37 <https://doi.org/10.1007/s10562-009-0124-7>.  
38  
39  
40 (46) Singh, K.; Kukkar, D.; Singh, R.; Kukkar, P.; Bajaj, N.; Singh, J.; Rawat, M.; Kumar, A.; Kim, K.-  
41 H., In situ green synthesis of Au/Ag nanostructures on a metal-organic framework surface for  
42 photocatalytic reduction of p-nitrophenol. *J. Ind. Eng. Chem.* **2020**, *81*, 196-205.  
43 <https://doi.org/10.1016/j.jiec.2019.09.008>.  
44  
45  
46 (47) Duan, L.; Fu, R.; Xiao, Z.; Zhao, Q.; Wang, J.-Q.; Chen, S.; Wan, Y., Activation of aryl chlorides  
47 in water under phase-transfer agent-free and ligand-free Suzuki coupling by heterogeneous  
48 palladium supported on hybrid mesoporous carbon. *ACS Catal.* **2015**, *5* (2), 575-586.  
49 <https://doi.org/10.1021/cs501356h>.  
50  
51  
52 (48) Klinkova, A.; Ahmed, A.; Choueiri, R. M.; Guest, J. R.; Kumacheva, E., Toward rational design of  
53 palladium nanoparticles with plasmonically enhanced catalytic performance. *RSC Adv.* **2016**, *6* (53),  
54 47907-47911. <https://doi.10.1039/C5RA25571F>.  
55  
56  
57  
58  
59  
60

- 1  
2  
3 (49) Dong, Z.; Le, X.; Liu, Y.; Dong, C.; Ma, J., Metal organic framework derived magnetic porous  
4 carbon composite supported gold and palladium nanoparticles as highly efficient and recyclable  
5 catalysts for reduction of 4-nitrophenol and hydrodechlorination of 4-chlorophenol. *J. Mater. Chem.*  
6 **A** **2014**, 2 (44), 18775-18785. <https://doi.org/10.1039/C4TA04010D>.  
7  
8  
9 (50) Pandey, S.; Mishra, S. B., Catalytic reduction of p-nitrophenol by using platinum nanoparticles  
10 stabilised by guar gum. *Carbohydr. Polym.* **2014**, 113, 525-531.  
11 <https://doi.org/10.1016/j.carbpol.2014.07.047>.  
12  
13 (51) Niu, W.; Li, Z.-Y.; Shi, L.; Liu, X.; Li, H.; Han, S.; Chen, J.; Xu, G., Seed-mediated growth of  
14 nearly monodisperse palladium nanocubes with controllable sizes. *Cryst. Growth Des.* **2008**, 8 (12),  
15 4440-4444. <https://doi.org/10.1021/cg8002433>.  
16  
17 (52) Hyotanishi, M.; Isomura, Y.; Yamamoto, H.; Kawasaki, H.; Obora, Y., Surfactant-free synthesis of  
18 palladium nanoclusters for their use in catalytic cross-coupling reactions. *Chem. Comm.* **2011**, 47  
19 (20), 5750-5752. <https://doi.org/10.1039/C1CC11487E>.  
20  
21 (53) Mandali, P. K.; Chand, D. K., Palladium nanoparticles catalyzed Suzuki cross-coupling reactions  
22 in ambient conditions. *Catal. Commun.* **2013**, 31, 16-20.  
23 <https://doi.org/10.1016/j.catcom.2012.10.020>.  
24  
25 (54) Vibhute, S. P.; Mhaldar, P. M.; Shejwal, R. V.; Pore, D. M., Magnetic Nanoparticles-Supported  
26 Palladium catalyzed Suzuki-Miyaura Cross Coupling. *Tetrahedron Lett.* **2020**, 151594.  
27 <https://doi.org/10.1016/j.tetlet.2020.151594>.  
28  
29 (55) Li, Y.; Xu, L.; Xu, B.; Mao, Z.; Xu, H.; Zhong, Y.; Zhang, L.; Wang, B.; Sui, X., Cellulose sponge  
30 supported palladium nanoparticles as recyclable cross-coupling catalysts. *ACS Appl. Mater.*  
31 *Interfaces* **2017**, 9 (20), 17155-17162. <https://doi.org/10.1021/acsami.7b03600>.  
32  
33 (56) Goksu, H.; Zengin, N.; Karaosman, A.; Sen, F., Highly active and reusable Pd/AlO (OH)  
34 nanoparticles for the Suzuki cross-coupling reaction. *Current Organocatalysis* **2018**, 5 (1), 34-41.  
35 <https://doi.org/10.2174/2213337205666180614114550>.  
36  
37 (57) Cargnello, M.; Wieder, N. L.; Canton, P.; Montini, T.; Giambastiani, G.; Benedetti, A.; Gorte, R.  
38 J.; Fornasiero, P., A versatile approach to the synthesis of functionalized thiol-protected palladium  
39 nanoparticles. *Chem. Mater.* **2011**, 23 (17), 3961-3969. <https://doi.org/10.1021/cm2014658>.  
40  
41 (58) Zeltner, M.; Schätz, A.; Hefti, M. L.; Stark, W. J., Magnetothermally responsive C/Co@ PNIPAM-  
42 nanoparticles enable preparation of self-separating phase-switching palladium catalysts. *J. Mater.*  
43 *Chem.* **2011**, 21 (9), 2991-2996. <https://doi.org/10.1039/C0JM03338C>.  
44  
45  
46  
47  
48  
49  
50  
51  
52  
53  
54  
55  
56  
57  
58  
59  
60

- 1  
2  
3 (59) Singh, A. S.; Shelkar, R. S.; Nagarkar, J. M., Palladium (II) on functionalized NiFe<sub>2</sub>O<sub>4</sub>: An  
4 efficient and recyclable phosphine-free heterogeneous catalyst for Suzuki coupling reaction. *Catal.*  
5 *Lett.* **2015**, *145* (2), 723-730. <https://doi.org/10.1007/s10562-014-1455-6>.  
6  
7  
8 (60) Kong, X.; Zhu, H.; Chen, C.; Huang, G.; Chen, Q., Insights into the reduction of 4-nitrophenol to  
9 4-aminophenol on catalysts. *Chem. Phys. Lett.* 2017, *684*, 148-152. [http://dx.doi.org/10.1016/](http://dx.doi.org/10.1016/j.cplett.2017.06.049)  
10 [j.cplett.2017.06.049](http://dx.doi.org/10.1016/j.cplett.2017.06.049).  
11  
12  
13 (61) Wang, Z.; Xu, C.; Gao, G.; Li, X., Facile synthesis of well-dispersed Pd-graphene nanohybrids and  
14 their catalytic properties in 4-nitrophenol reduction. *RSC Adv.* **2014**, *4* (26), 13644-13651.  
15 <https://doi.10.1039/C3RA47721E>.  
16  
17  
18 (62) Venkatesham, M.; Ayodhya, D.; Veerabhadram, G., Green synthesis, characterization and catalytic  
19 activity of palladium nanoparticles by xanthan gum. *Appl. Nanosci.* **2015**, *5* (3), 315-320.  
20 <https://doi.org/10.1007/s13204-014-0320-7>.  
21  
22  
23 (63) Zhu, Y.; Wang, W. D.; Sun, X.; Fan, M.; Hu, X.; Dong, Z., Palladium nanoclusters confined in  
24 MOF@ COP as a novel nanoreactor for catalytic hydrogenation. *ACS Appl. Mater. Interfaces* **2020**.  
25 <https://doi.org/10.1021/acsami.9b21802>.  
26  
27  
28 (64) Gu, X.; Qi, W.; Xu, X.; Sun, Z.; Zhang, L.; Liu, W.; Pan, X.; Su, D., Covalently functionalized  
29 carbon nanotube supported Pd nanoparticles for catalytic reduction of 4-nitrophenol. *Nanoscale*  
30 **2014**, *6* (12), 6609-6616. <https://doi.org/10.1039/C4NR00826J>.  
31  
32  
33  
34  
35  
36  
37  
38  
39  
40  
41  
42  
43  
44  
45  
46  
47  
48  
49  
50  
51  
52  
53  
54  
55  
56  
57  
58  
59  
60

**For Table of Contents Use Only**